Superconducting Magnet Systems for the Muon-Electron Conversion Experiment

Bradford A. Smith, *Member, IEEE*, Alexi Radovinsky, Peter H. Titus, Joseph L. Smith, John G. Brisson, Joseph V. Minervini, Joel H. Schultz, Richard J. Camille, Jr., William R. Molzon, Michael Hebert, T. J. Liu, and William V. Hassenzahl

***Abstract*—The Muon-to-Electron Conversion Experiment (MECO) seeks to detect muon to electron conversion, providing evidence that the conservation of muon and electron type lepton number can be violated. Observation of this violation would suggest physics beyond the Standard Model. The experiment is to be installed at Brookhaven National Laboratory (BNL). A high energy proton beam produces pions upon hitting a heavy target inside the 1.5 m diameter by 5 m long Production Solenoid (PS). A fraction of the muons from pion decay are captured in the 0.5 m diameter bore by the 13 m long, S-shaped Transport Solenoid (TS), which contains collimators, providing sign and momentum selection. The muons are stopped in a target inside a 1.9 m bore by 10 m long Detector Solenoid (DS) that houses detectors to measure the energy of the conversion electrons. Magnetic field is controlled to 5 T $\pm$5% at the high-field end of the PS and to 1 T $\pm$0.2% in the detector region of the DS. The conceptual design for the magnets is summarized, including conductor, coil, structure and cryogenic design.**

***Index Terms*—Detector magnets, superconducting cables, superconducting magnets.**

I. Introduction

MECO is one of two experiments comprising the Rare Symmetry Violating Processes (RSVP) initiative, a proposal [1] to the U. S. National Science Foundation by the collaborators. MECO is searching for the direct, neutrinoless conversion of a muon to an electron in the field of a nucleus at the unprecedented detection level of two out of 10^{17} stopped muons. This process has never been observed before, but is expected to occur in many theories that attempt to go beyond the present understanding of high energy physics. Observation of this process, and its rate of occurance, will go a long way toward determining which, if any, of these new theories is correct. The experiment will use an intense proton beam from the Alternating Gradient Synchrotron (AGS) at Brookhaven National Laboratory (BNL).

The superconducting solenoids form a large part of this experiment. The magnets create a specified magnetic field that varies nearly monotonically from 5 T in the Production Solenoid (PS) to 1 T in the Detector Solenoid (DS). Field is controlled over a volume around a curvilinear axis with a developed length of about 27 m (Fig. 1). Protons from the AGS strike a target inside the 1.5 m diameter warm bore of the PS, creating pions. The pions decay to muons, which follow the field lines through the 0.5 m diameter warm bore of the Transport Solenoid (TS), where they are filtered, via bending and collimation, and strike a target within the 1.9 m warm bore of the DS.

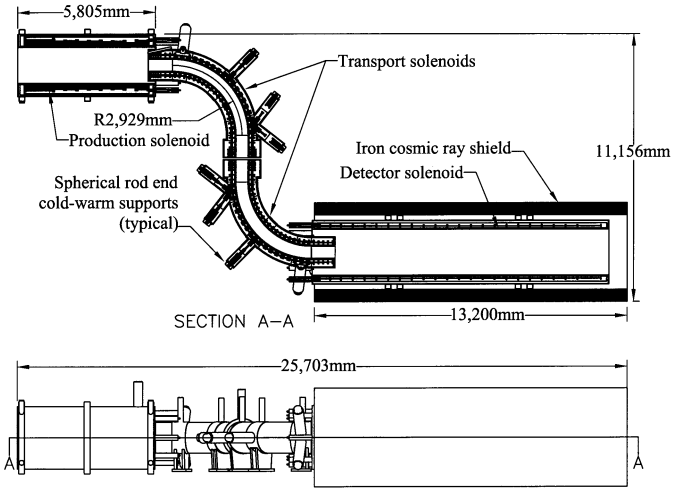

Fig. 1. Layout of the MECO solenoids.

The MIT Plasma Science and Fusion Center has completed a conceptual design for these solenoids, as described here.

II. Magnetic Field and Coils

Meeting the field specification imposed by the physics requirements is critical to MECO success. Fields range from 5 T to 2.5 T over 4 m in the PS, 2.5 m to 2 T over a developed length of 13.2 m in the TS, and from 2 T to 1 T over 10 m in the DS. Fields are specified over a volume limited by a surface formed by a circle of a variable radius, R_{fs}, normal to the S-shaped axis of the magnet system, as given in Table I. Each coil section has an associated length (L), a developed axial location $(Z\min, Z\max)$, specified R_{fs}, an allowed field deviation from the specification $(|\mathrm{delta}B/B|)$, and an allowed gradient of axial field along the axis (dB/ds).

Field matching involved an iterative approach. An initial coil configuration (geometry, ampere turns and coil count), is postulated, fields are solved at specific points along a mid-plane path in the field volume with a 1 : 1 relation between coil and field

Manuscript received August 6, 2002. This work was supported in part by the National Science Foundation under Grant 0100566–0013144000 and by the Department of Energy under Grant DE-FG04-91ER40679.

B. A. Smith, A. Radovinsky, P. H. Titus, J. L. Smith, J. G. Brisson, J. V. Minervini, and J. H. Schultz are with the Massachusetts Institute of Technology, Cambridge, MA 02139 USA (e-mail: smith@ psfc.mit.edu).

R. J. Camille, Jr., was with MTechnology, Inc. Saxonville, MA 01701 USA. He is now with Myatt Consulting, Inc., Norfolk, MA 02056 USA (e-mail: cryo.man@verizon.net).

W. R. Molzon, M. Hebert, and T. J. Liu are with the University of California, Irvine, CA 92697 USA (e-mail: wmolzon@uci.edu).

W. V. Hassenzahl is with Advanced Energy Analysis, Inc, Piedmont, CA 94611 USA (e-mail: advenergy1@aol.com).

Digital Object Identifier 10.1109/TASC.2003.812668

1051-8223/03$17.00 © 2003 IEEE

TABLE I
MAGNETIC FIELD SPECIFICATION

Coil	L	Zmin	Zmax	R_{fs}	|deltaB/B|		dB/ds**
	(m)	(m)	(m)	(m)	max	where	(T/m)
PS0	4.00	0.00	4.00	0.30	0.050	r=0	< 0
TS1	1.00	4.00	5.00	0.15	0.005	r=0	< -0.02
TS2	4.60*	5.00	9.60	0.15	0.010	$r<R_{fs}$	na
TS3	1.95	9.60	11.55	0.19	na	na	< -0.02
TS4	4.60*	11.55	16.15	0.15	0.010	$r<R_{fs}$	na
TS5	1.00	16.15	17.15	0.15	0.005	r=0	< -0.02
DS1	4.00	17.15	21.15	0.30-0.70	na	na	var< 5%
DS2	4.00	21.15	25.15	0.70	0.002	$r<R_{fs}$	na
DS3	2.00	25.15	27.15	0.70	0.010	$r<R_{fs}$	na

*Corresponds to R_{major} = 2.929 m
**where $r<R_{fs}$

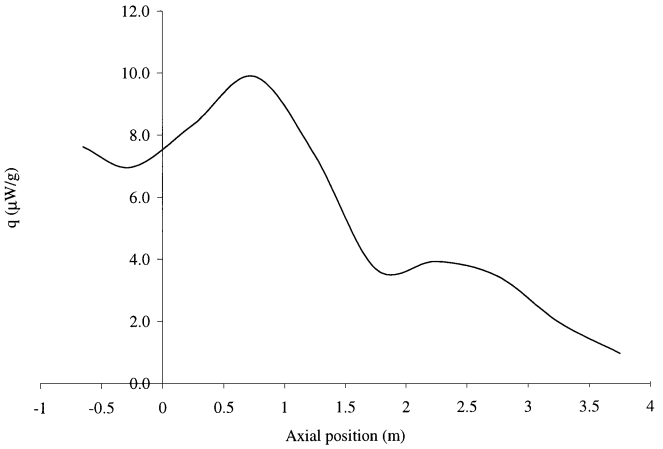

Fig. 2. Azimuthal peak nuclear heating in the PS vs. axial position. The field specification region begins at z $z = 0$; the PS winding begins at $z = -1$.

point counts. Current in each coil is solved based on the difference at each point between calculated field and specification. Adjustment for field from the iron around the DS is made with each iteration. Final evaluation uses actual coil current and conductor geometry to verify the calculated field against the specification at 1 cm intervals along the path. Ultimately, a total of 94 coils were found to provide a good match to the field requirement. There are 9 coils in the PS cryostat, 32 in the upstream TS cryostat (TSu), 30 in the downstream TS cryostat (TSd) and 23 in the DS cryostat.

A tolerance study was also done to evaluate sensitivity to individual coil-position misalignments (axial, transverse and angular), and to turn placement errors. The latter actually set the current limit in the DS and curved TS sections at 4000 A and at 1500 A in the TS straight sections. PS current is limited by conductor margin requirements (see below).

III. CONDUCTOR

MECO has been offered the use of sufficient quantities of SSC inner and outer cable to wind all solenoids. The conceptual design therefore concentrated on showing that SSC conductor can meet all requirements. Following a literature survey, MECO adopted a maximum fraction-of-critical current of 0.65 and minimum temperature margin of 1.5 K, to be met simultaneously by all conductors, joints and bus bars. For quench protection, MECO adopted a maximum allowable conductor temperature of 150 K, and a maximum dump voltage of 2 kV, subject to satisfying structural requirements during a quench. In addition, PS conductors sustain an azimuthal peak nuclear heating profile (Fig. 2).

Conductor designs meeting these criteria are given in Table II; terms are defined in Table III. SSC cables are soft soldered into half-hard, high conductivity copper channels sized for each coil section according to quench protection needs. Turn insulation is half-lapped, 0.025 mm thick Kapton tape, followed by half-lapped, 0.075 mm thick fiberglass tape.

IV. CONDUCTOR JOINTS AND LEADS

Conductor joints are needed between adjacent coils within a coil group (PS, TSu, TSd, or DS). Large coils may require joints

TABLE II
CONDUCTOR DESIGN FOR EACH COIL SECTION

	Units	PS coils	Up-stream TS in-line coils	Up-stream TS bend coils	Down-stream TS in-line coils	Down-stream TS bend coils	DS coils
SSC Cable Type		Inner	Outer	Outer	Outer	Outer	Outer
Energy	MJ	109	3.3	4.7	2.0	3.6	31
I_{op}	A	3500	1500	4000	1500	4000	4000
τ	s	34.7	2.41	1.31	1.49	0.99	8.54
A_{sc}	mm^2	6.21	4.29	4.29	4.29	4.29	4.29
J_{sc}	A/mm^2	564	350	933	350	933	933
A_{Cu_cable}	mm^2	8.07	7.71	7.71	7.71	7.71	7.71
w_{cond}	mm	14.53	13.60	13.60	13.60	13.60	15.00
h_{cond}	mm	4.40	2.40	2.40	2.40	2.40	2.80
A_{Cu_actual}	mm^2	48.5	21.0	21.0	21.0	21.0	30.3
$A_{inscond}$	mm^2	71.7	39.2	39.2	39.2	39.2	49.28
$J_{inscond}$	A/mm^2	48.8	38.3	102	38.3	102	81.2
J_{Cu}	A/mm^2	72.2	71.3	190	71.3	190	132
B_{max}	T	5.9	3.54	2.85	3.37	2.49	2.03
T_{op}	K	4.58	5.04	5.04	5.04	5.04	5.04
$J_c (T_{op}, B_{max})$	A/mm^2	1830	2880	3210	2960	3380	3600
f_c		0.31	0.12	0.29	0.12	0.28	0.26
TempMar	K	1.5	2.30	1.97	2.37	2.12	2.30

internal to the coil body. Conductor joints are lap joints with at least a two-conductor-twist-pitch overlap length to ensure temperature margins are met. Joint solder is Indalloy #8 with a liquidus/solidus temperature of 93 °C, well below the ∼188 °C melting temperature of the 60 Sn–40 Pb solder that bonds the cable in the channel. Joints in the PS, which is bath cooled by liquid helium, are bath cooled. TS and DS windings are conduction cooled. Their joints are in vacuum, but traced with liquid helium tubes. Leads are conventional vapor-cooled leads located outside the experimental shield wall, thus requiring approximately 10 m long superconducting bus between the leads and the coils. Buses will be bath cooled (PS) or traced with helium tubing in vacuum (TS and DS).

TABLE III
PARAMETER DEFINITIONS FOR TABLE II

Parameter	Definition
Energy	stored energy in the coil set
I_{op}	operating current
τ	calculated time constant based on the stored energy, the operating current and setting V_{dump} = 1800 V
A_{sc}	non-copper area in the cable
J_{sc}	current density in the non-copper area
A_{Cu_cable}	Area of the copper in the cable
w_{cond}	overall width of the copper channel
h_{cond}	overall height of the copper channel
A_{Cu_actual}	sum of channel copper area + cable copper area
$A_{inscond}$	cross-sectional area of the insulated conductor
$J_{inscond}$	current density over the cross-sectional area of the insulated conductor
J_{cu}	current density when all current flows in the Acu_actual
B_{max}	peak field on the conductor in the coil set
T_{op}	operating temperature of the conductor at the peak field location
J_c	critical current at Top, Bmax
f_c	J_{op}/J_c
TempMar	$T_{cs} - T_{op}$, where T_{cs} is the current sharing temperature

TABLE IV
QUENCH ANALYSIS SUMMARY

Parameter	Units	PS	TS1	TS2	TS3u cable	DS
I, operating	A	3500	1500	4000	1500	4000
Stored energy	MJ	109	3.26	4.72	3.26	30.8
R_{dump}	Ohm	0.529	1.23	0.463	1.23	0.463
Time constant	s	33.64	2.36	1.27	2.36	8.32
Vmax coil	V	1900	1853	1876	1862	1863
Vmax, normal	V	532	4.6	41.4	27.4	145
R, normal zone	mOhm	427	5.3	17.9	70.8	118
T, hot spot	K	88.5	33	74.5	65.8	123
Energy dumped in coil	MJ	27.2	9.6e-3	175e-3	56e-3	2.69

V. QUENCH DETECTION AND PROTECTION

Quench detection is complex because no two coils within a coil group (PS, TSu, TSd, or DS) have the same geometry. Thus, balanced inductive voltages are unavailable for use in isolating the desired resistive voltage component. Furthermore, conceptual designers concluded the risk of shorts from co-winding a pick-up-wire in each coil for voltage cancellation is too high. Therefore, a digital quench protection system has been proposed, with a less-sensitive analog backup. Voltages measured on each coil are digitally corrected by dI/dt-proportional signals from each coil set. The system is calibrated at installation during charge and discharge.

A three-dimensional quench code developed at MIT-PSFC calculates coil temperature distributions as a function of time for the highest field coils within each coil group. Quench results are summarized in Table IV. Hot spot temperatures are well below the 150 K limit for all coil types, and coil voltages are below 2 kV. Also, the outer aluminum shells supporting the PS coils absorb 6.6 MJ of energy and reach a maximum temperature of about 53 K during the transient.

Temperature-time data are output for each quench model element and input to a structural analysis in ANSYS.

VI. COIL STRUCTURES

The MECO magnet system is divided into four magnet assemblies, each with it's own cryostat: PS, TSu, TSd and DS. These are based on ease of shipping, and natural boundaries formed by each magnet's function. Inter-assembly loads are reacted through cold mass supports to the facility foundation.

Both fusion project [2] and ASME criteria are used for guidance in coil structural design. Fusion criteria allow coil primary membrane stress to be based on the lesser of 2/3 of the Yield Strength (Sy) or 1/2 of the Ultimate Strength (Su) when coils are supported by cases. Otherwise, ASME Code criteria are used, which base the primary stress on 1/3 ultimate. For structural elements, ASME-like criteria are adopted with membrane stresses remaining below the maximum allowable stress, Sm, where Sm is the lesser of 2/3 of yield or 1/3 of ultimate. Bending discontinuity, and secondary stresses are treated in a manner similar to the ASME Code. Bolting and column buckling guidance is taken from AISC, with average net section bolt stresses kept below 0.6*yield. Yield and Tensile Strength properties are taken at the loaded temperature.

MECO is required to operate in several modes that include energizing any or all coil groups (PS, TS or DS) and having the magnet warm bores at atmosphere or vacuum. MECO structural design is based on meeting design criteria and various loading conditions. All windings have a low friction material between side flanges and coils.

Hoop loads in each PS coil are supported by an outer 6061 T6 aluminum mandrel which has an integral side flange and a bolted flange to facilitate coil assembly. Mandrels allow operation at a higher winding pack current density than otherwise possible for unsupported coils, and also provide winding axial pre-compression on cooldown. Axial pre-compression is needed to offset 45 MPa of axial tension that develops during quench in the largest, highest field PS coil. With a 0.5 mm radial assembly gap, maximum local stress in the winding is about 168 MPa, below the 200 MPa allowable for the average primary membrane stress for half-hard copper. Peak mandrel stresses depend on final assembly gaps and the as-built composite winding modulus, but remain below the 4 K allowable for several possibilities considered.

TS and DS coils are wound on internal stainless steel mandrels, are self supporting in hoop, and generally experience low axial and hoop stress due to lower fields. TS 90° bends are wound as right-circular solenoids on mandrels with tapered side flanges which are bolted together.

When all coils are all energized, there are attractive forces between the PS and TS of 1.2 MN, and between the TS and DS of 0.69 MN. The 90° bends of the TS also experience centering loads. These and the vertical loads are reacted by different cross-sectional-area sets of 316 LN spherical-end struts which handle small rotations during cooldown and Lorentz loading. The struts work either in tension only or in tension-compression opposition with outer structural cylinders which form the cryostat vacuum boundary. TS-bend coil stresses are highest below the attachments for the struts, but within allowable values. Outer vacuum shells of all cryostats have local reinforcement rings to carry the inter-coil and gravity loads to the facility floor. The

struts also permit final adjustment of coil assembly positions by up to a few centimeters during magnet installation. Finite element models of cooldown and operational displacements should enable prediction of warm-temperature component fabrication and assembly locations to within a few millimeters.

All cryostats are made from stainless steel and are designed to carry the vacuum loads. The PS cryostat inner vacuum can is 2 cm thick and can carry the 65 000 kg radiation shield. Each TS cryostat has a 1-m-long straight section at each end, which carries a 1200 kg collimator on its 1-cm-thick inner wall. The DS cryostat inner vacuum can is 1 cm thick and carries 4250 kg of local loads and 6800 kg of distributed loads from mounted experimental equipment.

VII. Cryostats, Control Dewars and Cryogenics

With 192 W (maximum) nuclear heat load at 4.5 K into the PS cold mass, it is cooled by 2-phase, natural convection liquid helium (LHe) with low vapor content. PS coil flanges are grooved to vent helium from the bore to the annulus between the coil's grooved OD surface and the aluminum shell, which is also bored radially. These components are surrounded by the stainless steel, 6700-liter LHe can, which is itself enclosed by the liquid nitrogen (LN2)-traced thermal radiation shield, multi-layer insulation and the cryostat which forms the vacuum boundary. During a PS coil quench, all 6700 liters of LHe will be lost, while the 25 cm diameter vent stack keeps the internal pressure below 5 atmospheres.

Nuclear heating in the TS and DS coils is negligible. In addition, these coils operate with higher temperature margins because of lower magnetic fields. Thus, these coils are cooled conductively, which also minimizes helium loss should a coil quench. Each coil mandrel and side flange is lined with a 1.5 mm thick copper sheet, which works with circumferential, split copper ribs at each coil flange OD and a coil OD copper sheet, to conduct incoming thermal radiation to a helium-tubing-traced copper bridge that spans the top of each coil. The flow circuit for TS and DS coils is from the high pressure helium connection at the refrigerator/liquefier, through a J-T valve, through the condenser coil of the control dewar and then into the series connection of the helium tubes tracing the copper bridges. Two phase helium returned from the TS and DS coils is recondensed in the control dewar. Liquid from the recondensing control dewar is fed to the helium can enclosing the PS coil. Two-phase liquid is returned to a separate PS dewar. Both the PS and recondensing control dewars are outside the shield block wall surrounding the experiment. Liquid helium is distributed from the liquefier through liquid-nitrogen-shielded, vacuum-insulated transfer ducts.

Heat loads for the system are given in Table V.

TABLE V
MECO Magnet System Heat Loads

System component	Refrigeration at 4.5 K	Liquid helium consumption
	Watt	Liter/hour
TSu totals	20.18	17.6
Supports	12.8	
Valves	1.37	
Vacuum separators	0.86	
Thermal radiation from 80 K	1.96	
Conductor electrical joints (qty 35)	3.19	
Current leads		17.6
TSd totals	20.13	17.6
Supports	12.8	
Valves	1.37	
Vacuum separators	0.86	
Thermal radiation from 80 K	1.96	
Conductor electrical joints (qty 33)	3.14	
Current leads		17.6
DS totals	20.63	12.8
Supports	6.04	
Valves	1.37	
Vacuum separators	0.86	
Thermal radiation from 80 K	8.26	
Conductor electrical joints (qty 24)	4.10	
Current leads		12.8
Control dewar		1.3
PS totals	208.37	11.2
Supports	8.0	
Valves	2.99	
Vacuum separators	0.86	
Thermal radiation from 80 K	3.28	
High energy radiation	192	
Conductor electrical joints (qty 10)	1.24	
Current leads		11.2
PS dewar		1.3
GRAND TOTALS	269.31	61.8

The refrigerator/liquefier will be either a refurbished unit at BNL or purchased new to better match the final MECO requirements.

VIII. Summary

The conceptual design of the MECO solenoids has been described. Features include detailed field matching, SSC cables in copper channels operating up to 5.9 T, coil winding, quench detection and protection, and integrated structural and cryogenic designs that meet the design criteria.

References

[1] MECO and KOPIO Collaborations. (1999, October) Rare symmetry violating processes, "RSVP," A proposal to the national science foundation to construct the MECO and KOPIO experiments. [Online]. Available: http://meco.ps.uci.edu/RSVP/html.

[2] *Fusion Ignition Research Experiment Structural Design Criteria; Doc. no. 11*, _FIRE_-DesCrit_IZ_022 499.doc, February 1999.